

# PROCEEDINGS OF SPIE

SPIEDigitalLibrary.org/conference-proceedings-of-spie

## Investigations on phase conjugation based on nondegenerate four wave mixing in a Rb vapor cell

J. Zhao, Z. Zhou, P. D. Lett

J. Zhao, Z. Zhou, P. D. Lett, "Investigations on phase conjugation based on nondegenerate four wave mixing in a Rb vapor cell," Proc. SPIE 11700, Optical and Quantum Sensing and Precision Metrology, 1170021 (5 March 2021); doi: 10.1117/12.2586674

**SPIE.**

Event: SPIE OPTO, 2021, Online Only

# Investigations on phase conjugation based on nondegenerate four wave mixing in a Rb vapor cell

J. Zhao<sup>a</sup>, Z. Zhou<sup>a</sup>, and P. D. Lett<sup>a, b</sup>

<sup>a</sup>Joint Quantum Institute, National Institute of Standards and Technology and the University of Maryland, College Park, Maryland 20742, USA.

<sup>b</sup>Quantum Measurement Division, National Institute of Standards and Technology, Gaithersburg, Maryland, 20899, USA.

## ABSTRACT

Phase conjugation is an nonlinear effect that results from the four-wave-mixing process. This peculiar effect, in analogy to a mirror, reflects an incident beam in a way that the reflection constitutes the time-reversal of the original beam. By combining the phase conjugate mirror with ordinary mirrors, a special resonator, called phase conjugate resonator (PCR), is constructed. The phase conjugate resonator has been used in a wide range of applications, including phase aberration correction, image transmission, holography, and phase sensing using interferometers. Here, we explore theoretically the properties of phase conjugate mirror by investigating its action upon a variety of quantum states. In addition, we analyze the input-output relations of a phase conjugate resonator. Experimental results are reported that faithfully verify PCR's enhanced stability as compared to normal resonators. Furthermore, we observe a linewidth narrowing effect that is only present in the phase conjugate resonator.

**Keywords:** phase conjugation, four wave mixing, quantum optics

## 1. INTRODUCTION

Phase conjugation is a unique phenomenon that readily mimics Stoke's principle of time reversal.<sup>1</sup> It originates from the parametric interaction between optical waves through a third-order nonlinear medium. The nonlinear medium constitutes a phase conjugate mirror (PCM) that distinctively differs from an ordinary mirror – while it inverts the propagation direction of the incident beam, it retains exactly the phase front feature of the incoming beam. PCMs have attracted a great deal of attention both theoretically and experimentally. It has been used widely to remove aberrations of wavefronts, which makes it a compelling tool to improve the fidelity of image and other signal transmissions through dispersive media.<sup>2–8</sup> Interferometers comprised of phase conjugate mirrors are shown to be more resilient to ambient phase noise.<sup>6</sup> Aside from the aforementioned numerous applications of a phase conjugate mirror, it can also be used to form a phase conjugate resonator (PCR) built with a PCM and an ordinary mirror.<sup>9–11</sup> Hybrid resonators that combines multiple PCMs and ordinary mirrors in different configurations have been investigated with respect to their intra-cavity fields and oscillation conditions.<sup>12–15</sup> The PCR and its variants were proved to be unconditionally stable;<sup>9, 11</sup> it mitigates the need for longitudinal-mode conditions, due to the fact that there is no net phase accumulated per round trip as would otherwise be  $2kL$  for a normal Fabry-Perot resonator with cavity length of  $L$ . The phase conjugate resonator has been utilized to realize narrow-band optical filtering,<sup>16</sup> optical imaging and holography.<sup>17, 18</sup> Other phenomenon such as chaos has also been observed in such systems.<sup>19, 20</sup>

Although the classical behavior of PCMs and PCRs has been studied extensively, studies about its effect on quantum states is yet limited to single-mode input.<sup>21</sup> Therefore, there remains an incentive to explore how it acts on other quantum states and whether or not it can produce some exotic nonclassical states. We first theoretically study the phase conjugate mirror acting on Gaussian and non-Gaussian quantum states. We also provide a

---

Further author information: (Send correspondence to P. D. Lett)

P. D. Lett.: E-mail: lett@umd.edu, Telephone: 1 301-405-1124.

formalism to investigate the transformation of any quantum states as inputs of a phase conjugate resonator. We demonstrate experimentally a stable lasing process with the capability of eliminating slow disturbance through self-alignment. This process is only enabled by employing a phase conjugate resonator via four-wave-mixing in a Rb vapor cell. We compare this to the lasing process of a normal resonator.

## 2. PHASE CONJUGATE MIRROR ACTING ON QUANTUM STATES – GAUSSIAN

Suppose the incident and reflected beams of the phase conjugate mirror are denoted by  $\hat{a}_1$  and  $\hat{a}_2$ , the dynamics of the PCM can be obtained by solving the Heisenberg equations of motions for  $\hat{a}_1, \hat{a}_2$ , following the four-wave-mixng (FWM) Hamiltonian

$$\mathcal{H}_{\text{FWM}} = i\hbar\chi\hat{a}_0^2\hat{a}_1^\dagger\hat{a}_2^\dagger + \text{H.C.}, \quad (1)$$

In situations when the two pump beams are bright and no pump depletion is present, the pump operators  $\hat{a}_0$  can be replaced by a complex number  $\beta$  representing the pump's complex amplitude. This gives rise to the mode transformations via a PCM as follows:

$$\hat{a}_1(t) = \sqrt{G}\hat{a}_1(0) + \sqrt{G-1}\hat{a}_2^\dagger(0), \quad \hat{a}_2 = \sqrt{G-1}\hat{a}_1^\dagger(0) + \sqrt{G}\hat{a}_2(0), \quad (2)$$

where  $G = \cosh(\chi\beta^2 t)$  refers to the FWM gain that depends on the pump's intensity, the nonlinear coefficient of the medium, and the nonlinear interaction length/time.

### 2.1 Quadrature squeezed states

We first consider a quadrature-squeezed state,  $a_{\text{in}}$ , as input to the phase conjugate mirror. The state can be squeezed either in the amplitude or phase quadrature. Recall Eqs. 2, we then obtain the output of the PCM which takes the form

$$\hat{b} = \sqrt{G-1}\hat{a}_{\text{in}}^\dagger + \sqrt{G}\hat{a}_v. \quad (3)$$

Here  $\hat{a}_v$  represents the vacuum noise coupled into the output through the PCM, in compliance with the commutation relation  $[\hat{b}, \hat{b}^\dagger] = 1$ . The variances of the amplitude and phase quadratures of the output state are

$$\langle (\Delta X_b)^2 \rangle = (G-1)\langle (\Delta X_{in})^2 \rangle + G, \quad (4)$$

$$\langle (\Delta Y_b)^2 \rangle = (G-1)\langle (\Delta Y_{in})^2 \rangle + G. \quad (5)$$

Consider an amplitude-squeezed input state, the output variance for the amplitude quadrature is lower bounded by

$$\langle (\Delta X_b)^2 \rangle \geq G + 1. \quad (6)$$

This means that regardless of the squeezing level of the input state, its quantum feature always vanishes due to the additional noise incurred on the PCM, as depicted in Fig. 2.1.

### 2.2 Quadrature EPR

In the following, we examine if the PCM is able to preserve the inseparability of an EPR state. The scattering matrix of the PCM can be written as

$$\Sigma_{\text{PCM}} = \begin{pmatrix} \sqrt{G} & 0 & 0 & \sqrt{G-1} \\ 0 & \sqrt{G} & \sqrt{G-1} & 0 \\ 0 & \sqrt{G-1} & \sqrt{G} & 0 \\ \sqrt{G-1} & 0 & 0 & \sqrt{G} \end{pmatrix} \quad (7)$$

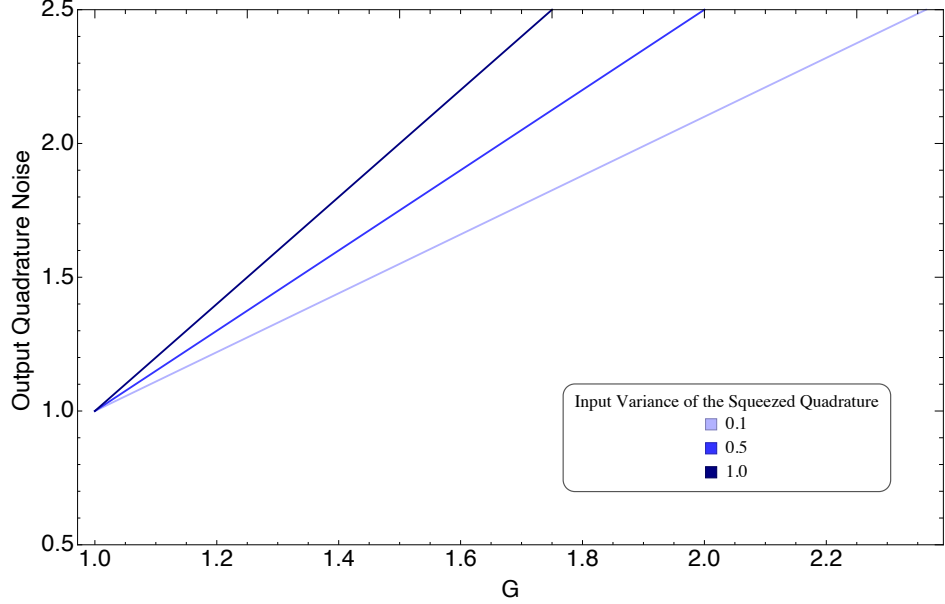


**Fig. 2.1** Output variance (normalized to shot noise) versus the PCM gain when a single-mode quadrature squeezed state is impinged onto the phase conjugate mirror.

Denote the covariance matrix of the input EPR as  $\Sigma_{\text{EPR}}$ , the output covariance matrix is determined by calculating  $(\Sigma_{\text{PCM}})^T \Sigma_{\text{EPR}} \Sigma_{\text{PCM}}$ .

$$\Sigma_{\text{out}} = \begin{pmatrix} \text{Cosh}(2r) & 0 & \sqrt{G}\text{Sinh}(2r) & 0 \\ 0 & \text{Cosh}(2r) & 0 & -\sqrt{G}\text{Sinh}(2r) \\ \sqrt{G}\text{Sinh}(2r) & 0 & G - 1 + G\text{Cosh}(2r) & 0 \\ 0 & -\sqrt{G}\text{Sinh}(2r) & 0 & G - 1 + G\text{Cosh}(2r) \end{pmatrix} \quad (8)$$

The parameter  $r$  quantifies the entanglement/squeezing level of the input EPR state. The resultant inseparability parameter of the output can be derived as

$$\begin{aligned} \langle \Delta(X_1 - X_2)^2 \rangle + \langle \Delta(Y_1 + Y_2)^2 \rangle = \\ 2\text{Cosh}(2r) + 2(G - 1) + 2G\text{Cosh}(2r) - 4\sqrt{G}\text{Sinh}(2r). \end{aligned} \quad (9)$$

Recall the inseparability criterion for a two-mode EPR state

$$\langle \Delta(X_1 - X_2)^2 \rangle + \langle \Delta(Y_1 + Y_2)^2 \rangle < 1/2. \quad (10)$$

In Fig. 2.2, we plot the output inseparability parameter as a function of the PCM gain. Note that unlike the situation where the PCM contaminates completely the quantum property of a single-mode quadrature squeezed state, the inseparability of the EPR state is preserved in certain circumstances. More specifically, we derive that in order for a PCM to preserve the inseparability of an incident EPR state, its gain must satisfy the following condition:

$$G < 1 - \frac{1}{8}\text{Sech}(r)^2(7 + 4\sqrt{2}\text{Sinh}(r)). \quad (11)$$

### 2.3 Intensity EPR

Consider the following situation where we generate twin beams from FWM that show intensity squeezing. We then send one of the twin beams onto a PCM. Suppose the initial input mode to the first FWM interaction is

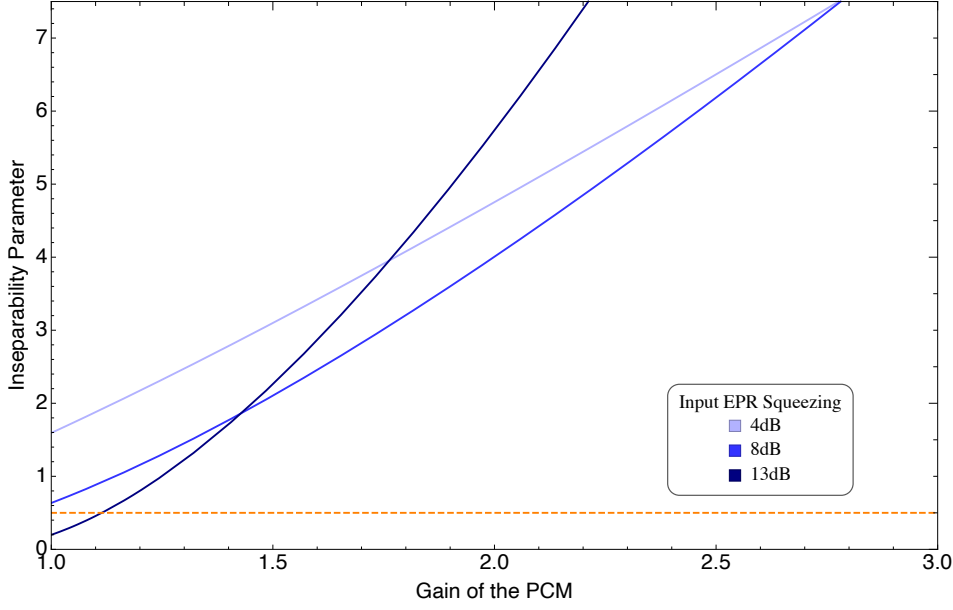


**Fig. 2.2** Output inseparability parameter as one arm of an EPR state is incident onto the phase conjugate mirror. We considered three input EPR squeezing levels: 4 dB, 8 dB, and 13 dB, respectively, shown in light to darker blue. The orange dashed line denotes the inseparability bound where the region above it represents classical separable states.

$\hat{a}_{\text{in}}$ , the output modes of the PCM can be represented by

$$\hat{a}_{o1} = \sqrt{G_1} \hat{a}_{\text{in}} + \sqrt{G_1 - 1} \hat{a}_{v1}^\dagger, \quad (12)$$

$$\hat{a}_{o2} = \sqrt{G_2(G_1 - 1)} \hat{a}_{\text{in}}^\dagger + \sqrt{G_1 G_2} \hat{a}_{v1} + \sqrt{G_2 - 1} \hat{a}_{v2}^\dagger. \quad (13)$$

Here,  $G_1$  and  $G_2$  are the gains of the FWM for twin-beam generation and the PCM, respectively. To calculate the intensity correlation between the two output modes, we first derive the photon number operators of the two modes by linearizing the creation and annihilation operators around their steady states.

$$\begin{aligned} \hat{a}_{o2}^\dagger \hat{a}_{o1} &= G_1(G_2 - 1)(\alpha_{\text{in}}^2 \\ &+ \alpha_{\text{in}} \delta X_{\text{in}}) + \sqrt{G_2(G_1 - 1)}(G_2 - 1)\alpha_{\text{in}} \delta X_{v1} \\ &+ \sqrt{G_1 G_2(G_2 - 1)}\alpha_{\text{in}} \delta X_{v2}, \end{aligned} \quad (14)$$

and

$$\begin{aligned} \hat{a}_{o1}^\dagger \hat{a}_{o1} &= G_1(\alpha_{\text{in}}^2 + \alpha_{\text{in}} \delta X_{\text{in}}) \\ &- \sqrt{G_1(G_1 - 1)}\alpha_{\text{in}} \delta X_{v1}. \end{aligned} \quad (15)$$

The mean photon number contained in the two output modes can be obtained:

$$\langle \hat{a}_{o2}^\dagger \hat{a}_{o2} \rangle = G_2(G_1 - 1)\alpha_{\text{in}}^2, \quad \langle \hat{a}_{o1}^\dagger \hat{a}_{o1} \rangle = G_1\alpha_{\text{in}}^2. \quad (16)$$

And the variance of the difference photon number operator can be expressed as:

$$\langle \delta \hat{N}_- \delta \hat{N}_- \rangle = \alpha_{\text{in}}^2 [G_1(1 + 2G_1(G_2 - 1) - 2G_2)(G_2 - 1) + G_2]. \quad (17)$$

Normalize this photon number noise to the shot noise that is given by

$$\text{SN} = [G_1 + G_2(G_1 - 1)] \alpha_{\text{in}}^2, \quad (18)$$

we obtain the output intensity difference noise:

$$SQ = \frac{G_1(1 + 2G_1(G_2 - 1) - 2G_2)(G_2 - 1) + G_2}{G_1 + G_2(G_1 - 1)}. \quad (19)$$

In Fig. 2.3, we plot the output intensity difference noise in dB. It is worthwhile noting that the intensity difference squeezing is significantly more resilient to the noise coupled through the back of the phase conjugate mirror, due to the fact that any common mode noise can be effectively eliminated by intensity subtractions.

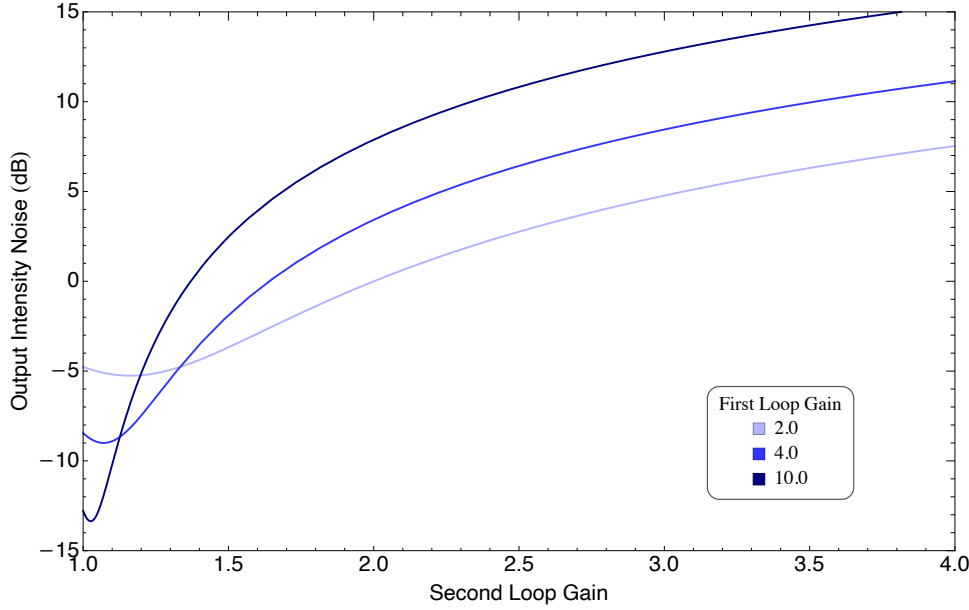


**Fig. 2.3** Output intensity difference noise for twin beam inputs.

### 3. PHASE CONJUGATE MIRROR ACTING ON QUANTUM STATES – NON-GAUSSIAN

In the following, we consider how the PCM acts upon two typical non-Gaussian states, i.e. single photon state and Schrödinger's cat state.

#### 3.1 Single photon

We first investigate how the PCM acts on a single photon state. Consider that a single photon state, as plotted in Fig. 3.1 is fed through the PCM. We denote the Wigner function of the input single photon state as  $W(\alpha_{\text{in}})$ , the Wigner function of the reflected mode is thus given by

$$\begin{aligned} W(\alpha_{\text{out}}) = & \\ & \int_{-\infty}^{\infty} dx_v dy_v W(\sqrt{G}x_v - \sqrt{G-1}x_{\text{out}}, \sqrt{G-1}y_{\text{out}} + \sqrt{G}y_v) \\ & W_{\text{vac}}(\sqrt{G}x_{\text{out}} - \sqrt{G-1}x_v, \sqrt{G}y_{\text{out}} + \sqrt{G-1}y_v) \end{aligned} \quad (20)$$

$W_{\text{vac}}(\alpha)$  here represents the vacuum mode coupled in through the PCM. Figure 3.2 showcases the output states for a variety of PCM gains. Note that the dip becomes smaller as the PCM gain increases. And more importantly, regardless of the gain value, the negative dip of the input single photon state always deteriorates by the additional noise introduced by the phase conjugation process. As a consequence, the outputs become purely classical states.

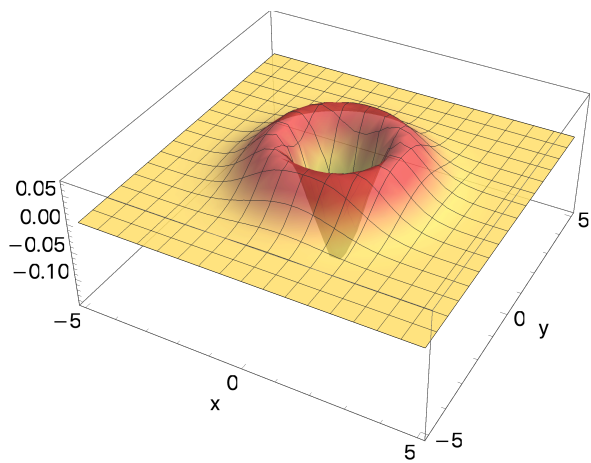


**Fig. 3.1** Wigner function of a single photon state as input to the PCM.

This result complements the experimental observations in Ref. [22] , where a very weak signal containing a few photons were sent through a PCM. The output energy density was constructed<sup>22</sup> ; however, to probe whether or not the negativity of a single photon state is preserved, a state tomography is required.

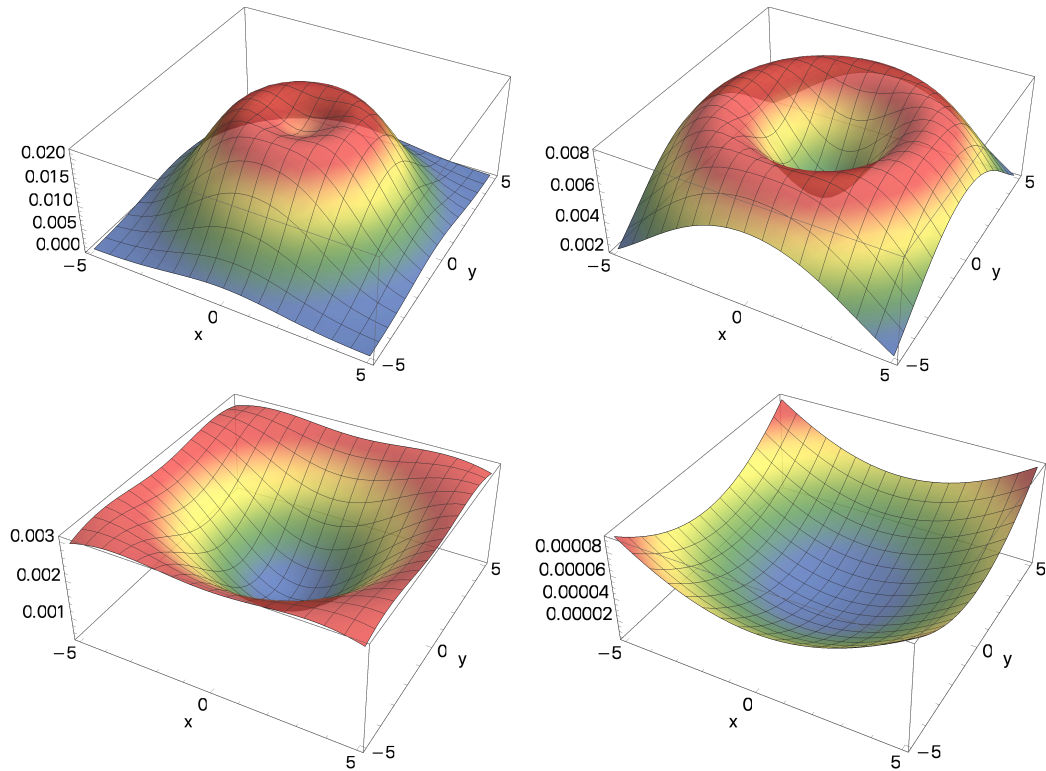


**Fig. 3.2** Output states for single-photon input at a variety of PCM gains:  $G = 2, 4, 10, 100$ .

### 3.2 Schrödinger's cat state

We now send a Schrödinger's cat state with an amplitude of 2.0 onto a PCM. The Wigner function of the input cat state is shown in Fig. 3.3. In Fig. 3.4, we present the ouput Wigner functions for  $G = 4.0$  and  $G = 10.0$ ,

respectively. Similar to the single photon case, the quantum feature, i.e. the negativity of the Wigner function is washed out by the phase conjugation.

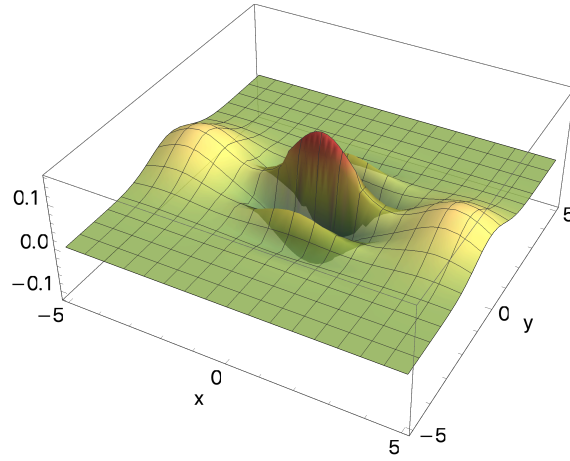


**Fig. 3.3** Input cat state.

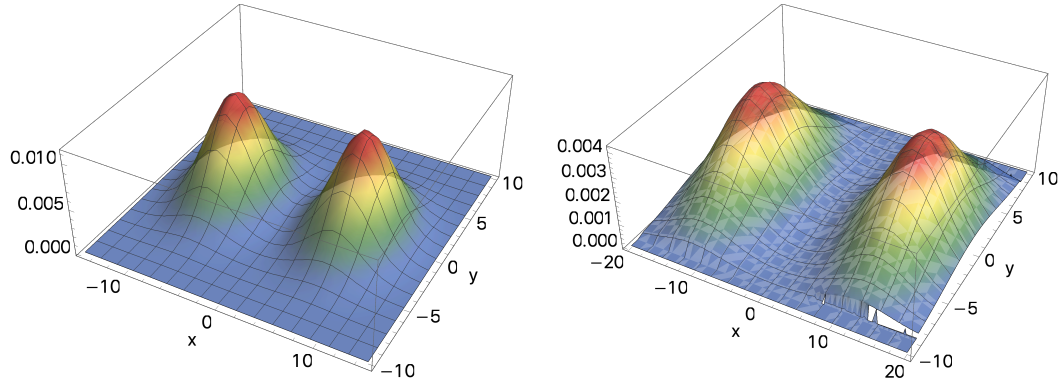


**Fig. 3.4** Output states for  $G = 4$  and  $G = 10$ .

#### 4. NONDEGENERATE PHASE CONJUGATE RESONATOR

The simplest phase conjugate resonator (PCR) is a one-sided cavity bounded by a phase conjugate mirror and an ordinary mirror as depicted in Fig. 4, where the reflectivity of M1 emulates the intra-cavity loss. The cavity is coherently driven by two pump fields that are counter-propagating to each other.  $\hat{A}_1$  and  $\hat{A}_2$  denote the probe and conjugate modes oscillating inside the resonator, whilst  $\delta\hat{A}_1^l$  and  $\delta\hat{A}_2^l$  represent the additional noise coupled into the resonator, attributed to cavity damping and intra-cavity loss.

##### 4.1 Classical Description

Consider two pump fields of frequency  $\omega_0$ , and a field of frequency  $\omega_0 + \omega_m$  that arises from the parametric upconversion of the pump beams and is injected into the phase conjugate resonator. The complex wavefunction of the beam is thus given by

$$\mathbf{E}_1(\mathbf{r}, t) \propto \mathbf{E}_1(\mathbf{r}) e^{i(\omega_0 + \omega_m)t}, \quad (21)$$

where  $\mathbf{E}_1(\mathbf{r})$  defines the transverse mode profile of the beam. As a result of the four wave mixing process, the phase conjugation of  $\mathbf{E}_1$  is produced when  $\mathbf{E}_1$  is impinged onto the phase conjugate mirror (PCM):

$$\mathbf{E}'_1(\mathbf{r}, t) \propto \mathbf{E}_1^*(\mathbf{r}) e^{i(\omega_0 - \omega_m)t}. \quad (22)$$

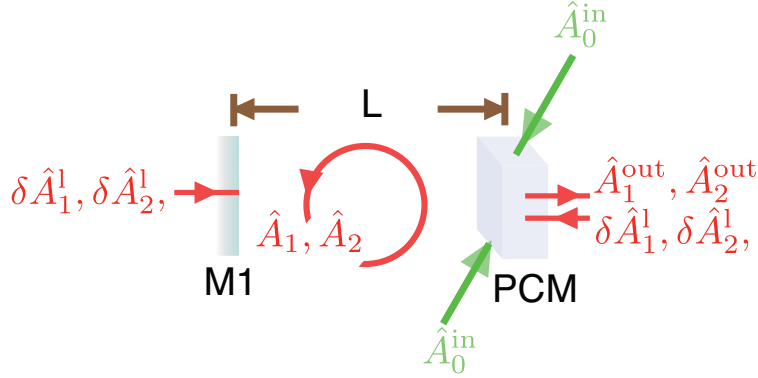


**Fig. 4** Conceptual scheme of a phase conjugate resonator.

The phase conjugated beam  $\mathbf{E}'_1$  travels one round trip inside the cavity, interacts with the two pump beams on the PCM, and hence reproduces the original mode  $\mathbf{E}_1$ . The input of the PCM thus can be expressed as the combination

$$\mathbf{E}(\mathbf{r}, t) = \mathbf{A} \left[ c_+ \mathbf{E}_1(\mathbf{r}) e^{i(\omega_0 + \omega_m)t} + c_- \mathbf{E}_1^*(\mathbf{r}) e^{i(\omega_0 - \omega_m)t} \right], \quad (23)$$

Here  $\mathbf{A} = A_0 \exp(i\theta_0)$  refers to the complex amplitude of the beam. Suppose the round trip transit time around the cavity from the PCM to mirror M1 and back is  $T = 2L/c$ , the cavity self-consistency condition requires that

$$\mathbf{E}(\mathbf{r}, t + T) = G \mathbf{E}'(\mathbf{r}, t), \quad (24)$$

where  $G$  is the net round-trip gain of the resonator. This condition results in the following relationships between the upshifted and the downshifted frequency components

$$c_+ = e^{-i\omega_m T} c_-^*, \quad c_- = e^{i\omega_m T} c_+^*. \quad (25)$$

Therefore, the resonant frequency shifting is fixed as  $\omega_m = n\pi/T$ , akin to the resonant longitudinal modes of a conventional cavity. And  $c_- = (-1)^n c_+^*$  always holds valid.

Without loss of generality, we assume that all the involved beams can be approximated by uniform plane waves propagating along the  $z$  axis and the coefficients  $c_+$  and  $c_-$  are real. The intra-cavity field can therefore be expressed as

$$\mathbf{E}_m(z, t) = \sum_m \mathbf{A} \left[ c_+ e^{-i\frac{2\pi}{\lambda_m} z} e^{i(\omega_0 + \omega_m)t} + c_- e^{i\frac{2\pi}{\lambda_m} z} e^{i(\omega_0 - \omega_m)t} \right] = \mathbf{A}'(t - \frac{z}{c}) e^{i\omega_0(t - \frac{z}{c}) + i\theta_0}, \quad (26)$$

where  $\mathbf{A}'$  is the complex envelope of the intra-cavity field that takes the form

$$\mathbf{A}'(t) = \sum_n A_0 c_+ \left( e^{\frac{in\pi t}{T}} + (-1)^n e^{\frac{-in\pi t}{T}} \right), \quad (27)$$

So the PCR has a central resonant frequency at the pump frequency of  $\omega_0$ . This cavity mode is surrounded by two comb sets, one centered at the probe frequency and the other centered at the conjugate frequency. The amplitudes of the comb sets are modulated by the FWM gain profile and the comb spacing is determined by the resonator self-consistency condition as  $1/2T = c/4L$ .<sup>9</sup>

The optical intensity of the beam is therefore

$$I(t, z) = |\mathbf{A}'(t, z)|^2 \quad (28)$$

$$= \sum_n A_0^2 c_+^2 [2 + 2\text{Cos}(n\pi - 2n\pi(t - z/c)/T)], \quad (29)$$

This resembles a Dirichlet Kernel with a period of  $T$ . This means that the PCM resonator works equivalently to a mode-locked laser that produces pulses at intervals of  $T$ . The pulse train alternates between the upshifting frequency components and the downshifting components at intervals of  $1/2T$ .

In order to study the probe/conjugate comb set, we investigate the optical intensity of the downshifting frequency components, whose complex envelope is given by

$$\mathbf{A}'_p(t) = \sum_{n=-s}^s A_0 c_+ e^{i\omega_m t} = \sum_{n=-s}^s A_0 c_+ \left( e^{i\frac{2\pi c}{4L}t} \right)^n. \quad (30)$$

The parameter  $s$  is related to the number of teeth in the probe comb set,  $M$ , by  $s = (M - 1)/2$ . It can be derived that

$$\mathbf{A}'_p(t) = A_0 c_+ \frac{\sin\left(\frac{\pi ctM}{4L}\right)}{\sin\left(\frac{\pi ct}{4L}\right)}. \quad (31)$$

The probe/conjugate pulse train therefore has a repetition rate of  $c/4L$  and pulse duration of  $4L/cM$ . The higher the number of modes, the shorter the pulse duration is.

## 4.2 Quantum Description

The PCR is conceptually equivalent to the coherent feedback/ feedforward scheme shown in Fig. 4.2. Its behavior can be described by a set of equations

$$\hat{b}_3 = \sqrt{G}\hat{a}_{\text{vin}2} + \sqrt{G-1}\hat{b}_2^\dagger, \quad (32)$$

$$\hat{a}_{\text{out}2} = \sqrt{G-1}\hat{a}_{\text{vin}2}^\dagger + \sqrt{G}\hat{b}_2, \quad (33)$$

$$\hat{b}_4 = e^{i\phi}\hat{b}_3, \quad \hat{b}_2 = e^{i\phi}\hat{b}_1, \quad (34)$$

$$\hat{b}_1 = \sqrt{G}\hat{a}_{\text{vin}1} + \sqrt{G-1}\hat{b}_4^\dagger, \quad (35)$$

$$\hat{a}_{\text{out}1} = \sqrt{G-1}\hat{a}_{\text{vin}1}^\dagger + \sqrt{G}\hat{b}_4, \quad (36)$$

where  $\phi$  denotes the phase delay introduced by the feedback loop. Here we assume the two loops have the same delay. The two output modes  $\hat{a}_{\text{out}1}$  and  $\hat{a}_{\text{out}2}$ , can therefore be obtained

$$\hat{a}_{\text{out}1} = \frac{e^{i\phi}G\hat{a}_{\text{vin}1} + 2\sqrt{G-1}\hat{a}_{\text{vin}2}^\dagger}{2-G}, \quad (37)$$

$$\hat{a}_{\text{out}2} = \frac{e^{i\phi}G\hat{a}_{\text{vin}2} + 2\sqrt{G-1}\hat{a}_{\text{vin}1}^\dagger}{2-G}. \quad (38)$$

Note that in the treatment presented here, we only consider a single mode of the probe and conjugate beams. One may generalize this formalism to accommodate the multi-mode situation by making a substitution of  $\hat{a} \rightarrow \sum_i \hat{a}_i$ , where  $\hat{a}_i$  represents different frequency modes.

## 5. EXPERIMENTAL RESULTS

Figure 5 (a) illustrates our experimental setup for constructing a phase conjugate resonator. A Ti-Sapphire laser is used to provide the light source. The laser is detuned by 800 MHz to the blue of the  $S_{1/2}(F=2) \rightarrow P_{1/2}(F'=3)$  transition in  $^{85}\text{Rb}$ . The laser output is fed through a 1.5 GHz acousto-optic-modulator (AOM) via a double-pass configuration to achieve a two-photon detuning of -2 MHz. This beam serves as the probe beam for the FWM process. First-order output of the AOM is sent to a reference cell to provide the saturated absorption spectroscopy, utilized to indicate the correct laser detuning. In order to obtain a bright pump beam, the zero-order output of the AOM is amplified by a tapered amplifier that gives rise to a pump beam with a power of 2 W. To maximize the FWM gain, the pump beam is aligned to possess a beam waist diameter of 1.5 mm,

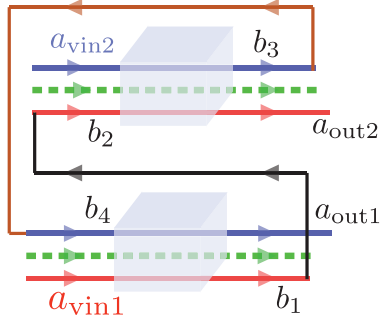


**Fig. 4.2** Unfolded scheme of a phase conjugate resonator. The green lines represent the pump beams for the FWM process, while the red and blue lines are the probe, and conjugate beams, respectively. The grey and the black lines denote the two feedback/feedforward loops.

whilst the probe beam has a beam waist diameter of  $700 \mu\text{m}$ . The two beams propagate across each other at the center of a 12mm Rb vapor cell at a small angle of approximately 0.3 to 0.5 degree. The intra-cavity lasing is initiated by the spontaneous emission of Rb atoms where two pump photons are converted to a probe photon and a conjugate photon, as shown in Fig. 5 (b). This parametric process acts as an phase conjugate mirror that transforms an incident optical field to its phase conjugation. Unlike using two counter-propagating pumps, or a self-pumped scheme, a single pump beam is employed in our scheme, which results in a nondegenerate PCR as described in Sec. 4. The resonator output is measured by beating it with a fraction of pump beam that has been down-shifted by 92 MHz. To demonstrate the unconditional stability of the PCR, we construct a normal resonator and compare its performance to the phase conjugate resonator under the same conditions.

In Fig. 5.2 (a) and 5.3 (a), we present the single-shot output noise spectra for the phase conjugate resonator and the normal resonator. Note that for the same feedback loop length, the linewidth of the lasing mode of the PCR is significantly narrower than that of a normal resonator. In addition, the measured output is also averaged for 60 s and the output noise spectra are plotted in Fig. 5.2 (b) and 5.3 (b). Note that in the same time duration, the frequency drift of the lasing mode in a normal resonator is significantly larger than that in a PCR. This drift is largely caused by temperature fluctuation in the lab and other phase noise. This coincides with the theoretical expectations of the phase conjugate resonator.

In conclusion, we provide theoretical descriptions of a phase conjugate mirror acting on various quantum states. In addition, we analyze the transformation of field operators as inputs to a phase conjugate resonator. Experimental results are reported that faithfully verify PCR's enhanced stability as compared to normal resonators. Furthermore, we observe a linewidth narrowing effect that is only present in the phase conjugate resonator.

## ACKNOWLEDGMENTS

Research presented in this proceeding is supported by the Air Force Office of Scientific Research (AFOSR) under grant # FA9550-16-1-0423.

## REFERENCES

- [1] Jenkins, F. A. and White, H. E., [*Fundamentals of Optics*], McGraw Hill, New York (1957).
- [2] Feinberg, J. and Hellwarth, R. W., “Phase-conjugating mirror with continuous-wave gain,” *Opt. Lett.* **5**, 519–521 (Dec 1980).
- [3] Levenson, M. D., “High-resolution imaging by wave-front conjugation,” *Opt. Lett.* **5**, 182–184 (May 1980).
- [4] Feinberg, J., “Self-pumped, continuous-wave phase conjugator using internal reflection,” *Opt. Lett.* **7**, 486–488 (Oct 1982).

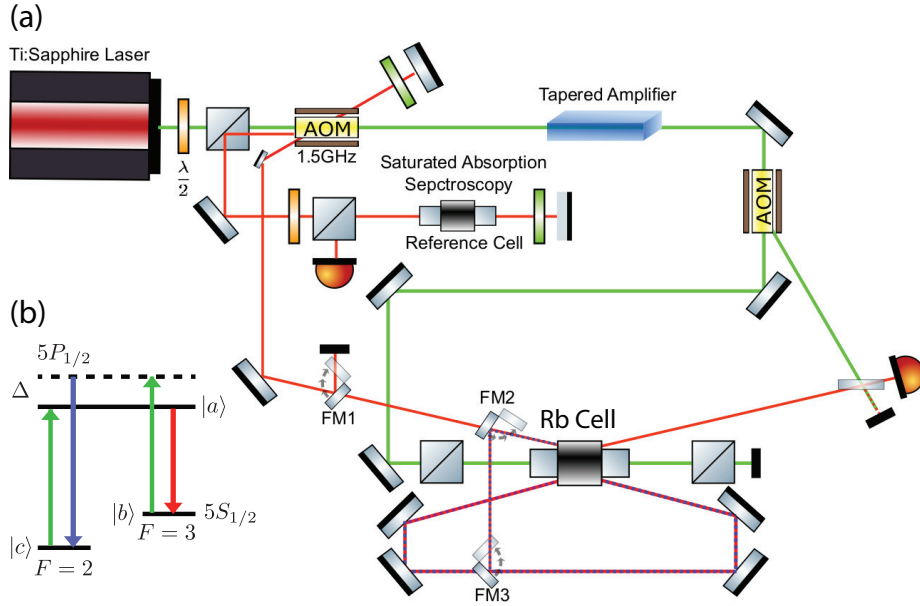


**Fig. 5** (a) Experimental scheme. FM: flip mirrors. The flip mirror FM1 is flipped down in the alignment stage; FM2 and FM3 are flipped down in pairs when constructing a normal resonator, and up in pairs when constructing a phase conjugate resonator. (b) Four-wave-mixing scheme in a hot Rb vapour. The pump photons are annihilated in the parametric process, accompanied by the creations of one probe photon and one conjugate photon, in compliance with energy and momentum conservation.

- [5] Lind, R. C. and Steel, D. G., “Demonstration of the longitudinal modes and aberration-correction properties of a continuous-wave dye laser with a phase-conjugate mirror,” *Opt. Lett.* **6**, 554–556 (Nov 1981).
- [6] Fischer, B. and Sternklar, S., “Image transmission and interferometry with multimode fibers using self-pumped phase conjugation,” *Applied Physics Letters* **46**(2), 113–114 (1985).
- [7] Ruan, H., Jang, M., and Yang, C., “Optical focusing inside scattering media with time-reversed ultrasound microbubble encoded light,” *Nature Communications* **6**(1), 8968 (2015).
- [8] Liu, X., Chraplyvy, A. R., Winzer, P. J., Tkach, R. W., and Chandrasekhar, S., “Phase-conjugated twin waves for communication beyond the kerr nonlinearity limit,” *Nature Photonics* **7**(7), 560–568 (2013).
- [9] Bélanger, P. A., Hardy, A., and Siegman, A. E., “Resonant modes of optical cavities with phase-conjugate mirrors,” *Appl. Opt.* **19**, 602–609 (Feb 1980).
- [10] Friberg, A. T., Kauranen, M., and Salomaa, R., “Dynamics of fabry-perot resonators with a phase-conjugate mirror,” *J. Opt. Soc. Am. B* **3**, 1656–1672 (Dec 1986).
- [11] Lam, J. F. and Brown, W. P., “Optical resonators with phase-conjugate mirrors,” *Opt. Lett.* **5**, 61–63 (Feb 1980).
- [12] Anderson, D. Z., “Coupled resonators employing phase-conjugating and ordinary mirrors,” *Opt. Lett.* **9**, 417–419 (Sep 1984).
- [13] Ewbank, M. D., Yeh, P., Khoshnevisan, M., and Feinberg, J., “Time reversal by an interferometer with coupled phase-conjugate reflectors,” *Opt. Lett.* **10**, 282–284 (Jun 1985).
- [14] Cronin-Golomb, M., Fischer, B., Kwong, S.-K., White, J. O., and Yariv, A., “Nondegenerate optical oscillation in a resonator formed by two phase-conjugate mirrors,” *Opt. Lett.* **10**, 353–355 (Jul 1985).
- [15] Korwan, D. R. and Indebetouw, G., “Experimental modal analysis of the spatiotemporal dynamics of a linear photorefractive phase-conjugate resonator,” *J. Opt. Soc. Am. B* **13**, 1473–1481 (Jul 1996).
- [16] Nilsen, J., Gluck, N. S., and Yariv, A., “Narrow-band optical filter through phase conjugation by nondegenerate four-wave mixing in sodium vapor,” *Opt. Lett.* **6**, 380–382 (Aug 1981).

- [17] CroninGolomb, M., Fischer, B., Nilsen, J., White, J. O., and Yariv, A., "Laser with dynamic holographic intracavity distortion correction capability," *Applied Physics Letters* **41**(3), 219–220 (1982).
- [18] CroninGolomb, M., Fischer, B., White, J. O., and Yariv, A., "Passive phase conjugate mirror: Theoretical and experimental investigation," *Applied Physics Letters* **41**(8), 689–691 (1982).
- [19] Liu, S. R. and Indebetouw, G., "Periodic and chaotic spatiotemporal states in a phase-conjugate resonator using a Photorefractive BaTiO<sub>3</sub> phase-conjugate mirror," *J. Opt. Soc. Am. B* **9**(11), 1507–1520 (1992).
- [20] Valley, G. C. and Dunning, G. J., "Observation of optical chaos in a phase-conjugate resonator," *Opt. Lett.* **9**, 513–515 (Nov 1984).
- [21] Gaeta, A. L. and Boyd, R. W., "Quantum noise in phase conjugation," *Phys. Rev. Lett.* **60**, 2618–2621 (Jun 1988).
- [22] Andreev, N. F., Bespalov, V. I., Dvoretsky, M. A., and Pasmanik, G. A., "Phase conjugation of single photons," *IEEE Journal of Quantum Electronics* **25**(3), 346–350 (1989).

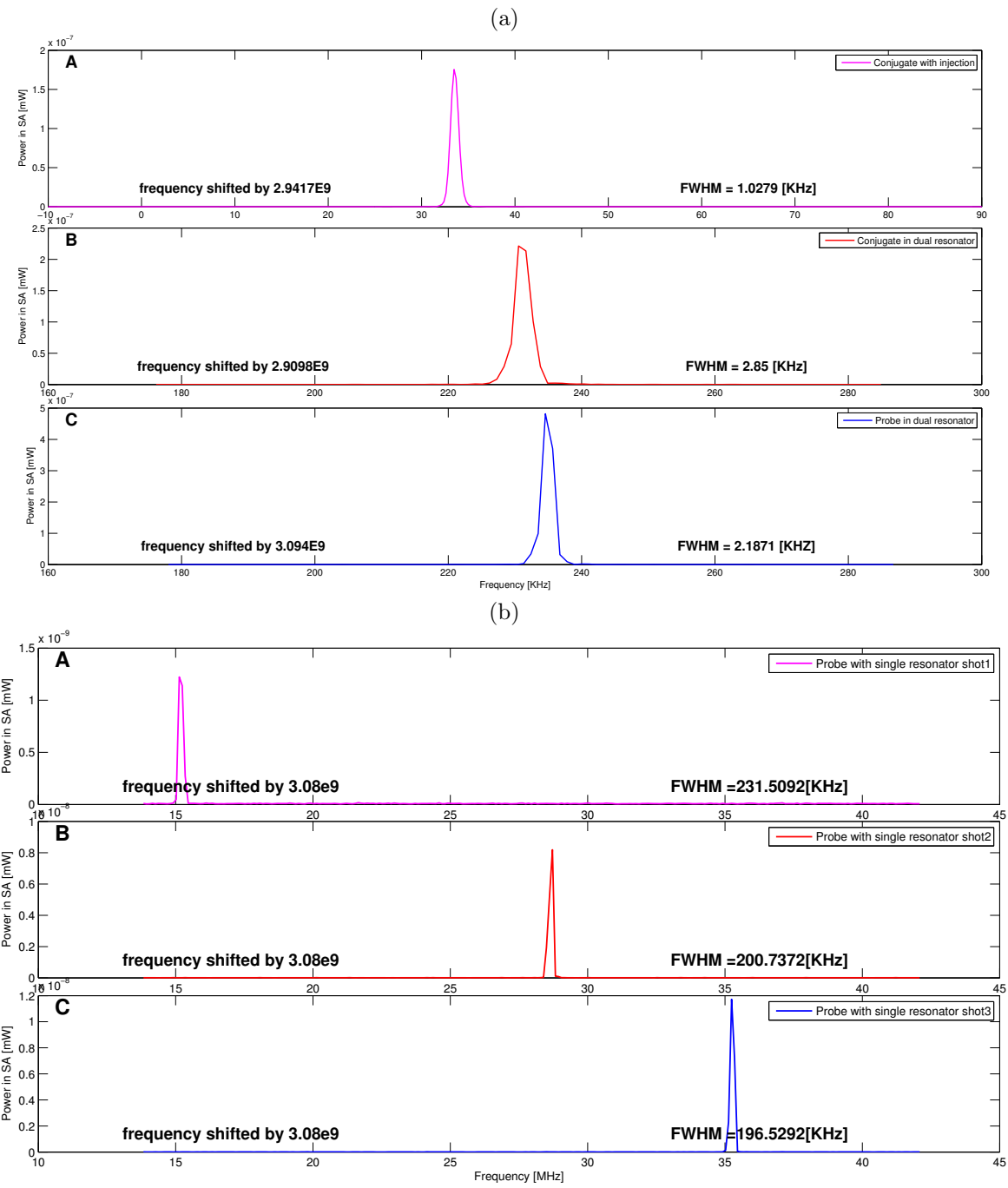


**Fig. 5.2** Single shot outputs for (a) the phase conjugate resonator and (b) the normal resonator. The noise spectra are obtained by beating the loop output with a fraction of the pump beam that is detuned by 92 MHz, as shown in Fig. 5. The normal resonator is constructed by flipping down FM2 and FM3 in Fig. 5 in conjunction with adding an etalon in the feedback loop that allows either probe or conjugate to pass through. Here we show the result when only probe beam is selected.

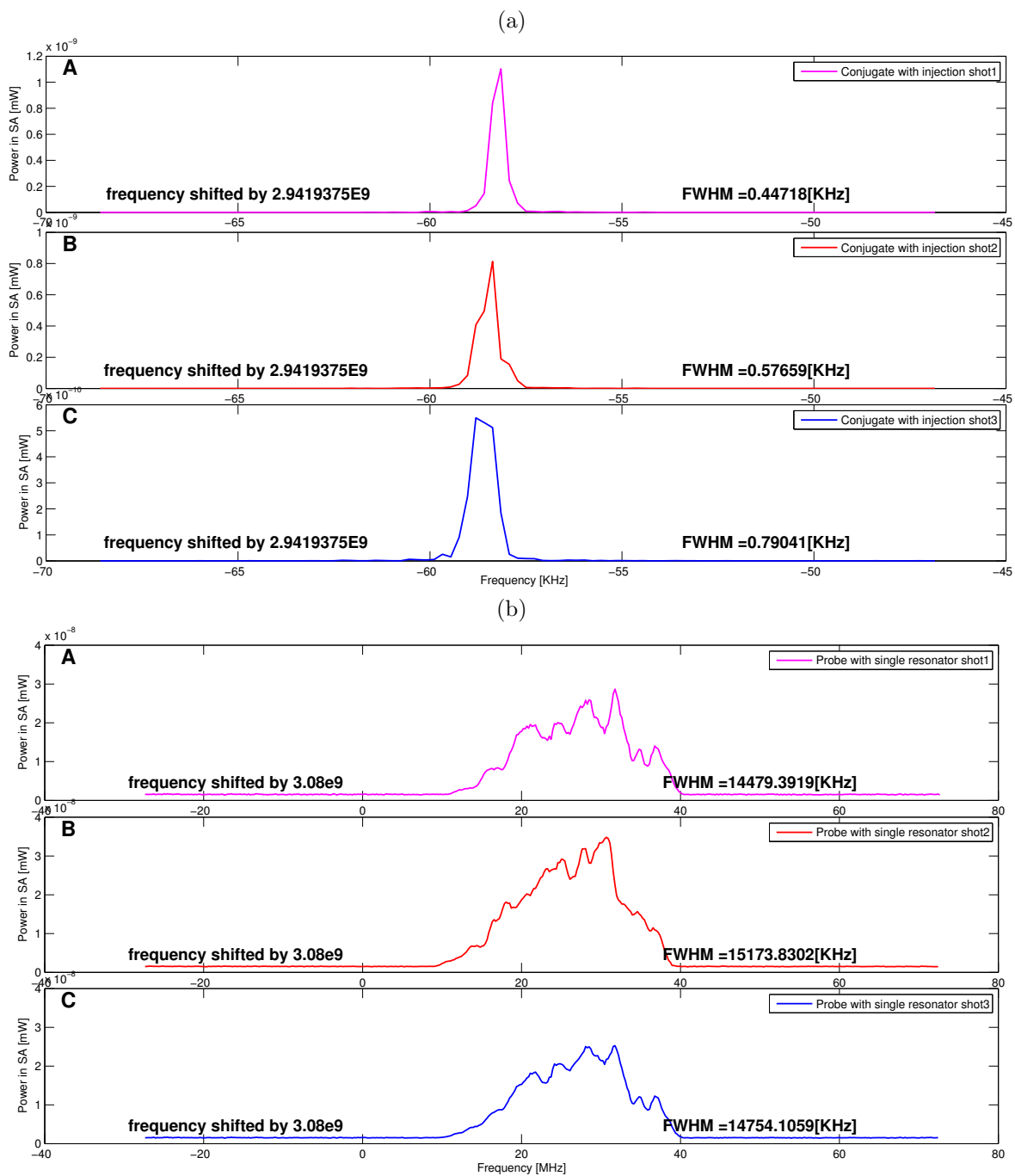


**Fig. 5.3** Output noise spectra averaged for 60 s for (a) the phase conjugate resonator and (b) the normal resonator. The noise spectra are obtained by beating the loop output with a fraction of the pump beam that is detuned by 92 MHz, as shown in Fig. 5.